New potential antitumoral di(hetero)arylether derivatives in the thieno[3,2-*b*]pyridine series: synthesis and fluorescence studies in solution and in nanoliposomes

Maria-João R. P. Queiroz,[a,*] Sofia Dias,[a] Daniela Peixoto,[a] Ana Rita O. Rodrigues,[b] Andreia D. S. Oliveira,[b] Paulo J. G. Coutinho,[b] Luís A. Vale-Silva,[c,d] Eugénia Pinto,[c,d] Elisabete M. S. Castanheira[b,*]

[a]*Departamento/Centro de Química, Universidade do Minho, Campus de Gualtar, 4710-057 Braga, Portugal*
[b]*Centro de Física (CFUM), Universidade do Minho, Campus de Gualtar, 4710-057 Braga, Portugal*
[c]*Laboratório de Microbiologia, Departamento de Ciências Biológicas, Faculdade de Farmácia da Universidade do Porto, Rua Aníbal Cunha 164, 4050-047 Porto, Portugal*
[d]*CEQUIMED-UP, Centro de Química Medicinal da Universidade do Porto, Rua Aníbal Cunha 164, 4050-047 Porto, Portugal.*

Abstract

New fluorescent methoxylated di(hetero)arylethers in the thieno[3,2-*b*]pyridine series were prepared by a copper-catalyzed Ullmann-type C-O coupling of the methyl 3-amino-6-bromothieno[3,2-*b*]pyridine-2-carboxylate with *ortho*, *meta* and *para*-methoxyphenols, using *N*,*N*-dimethylglycine as the ligand and Cs_2CO_3 as the base. The compounds obtained were tested for their inhibitory growth activity in three human tumor cell lines MCF-7 (breast adenocarcinoma), A375-C5 (melanoma), NCI-H460 (non-small cell lung cancer). The di(hetero)arylethers bearing a methoxy group in the *ortho* and *meta* positions showed very low GI_{50} values (1.1–2.5 μM) in all the three tumor cell lines. Their fluorescence properties in solution and when encapsulated in different nanoliposome formulations, composed either by egg-yolk phosphatidylcholine (Egg-PC), dipalmitoyl phosphatidylcholine (DPPC), dimyristoyl phosphatidylglycerol (DMPG), dioctadecyldimethylammonium bromide (DODAB), distearoyl phosphatidylcholine (DSPC), with or without cholesterol (Ch), or distearoyl phosphatidylethanolamine-(polyethylene glycol)2000 (DSPE-PEG), were studied. All compounds can be carried in the hydrophobic region of the liposome membrane. The liposomes with incorporated compounds are nanometric in size (diameter lower than 150 nm) and have generally low polydispersity.

Keywords: Ullmann-type C-O coupling; Di(hetero)aryleters; Thieno[3,2-*b*]pyridines; Fluorescence; Nanoliposomes

1. Introduction

Thienopyridine derivatives including di(hetero)arylethers have attracted much attention because of their potential different biological activities namely as antitumoral agents [1], nonreceptor Src kinase inhibitors [2] and receptor tyrosine kinase inhibitors [3,4,5].

Nanoliposomes are new technological developments for the encapsulation and delivery of bioactive agents. Because of their biocompatibility and biodegradability, along with their size, nanoliposomes have potential applications in a vast range of fields, including nanotherapy. Nanoliposomes are able to enhance the performance of bioactive agents by improving their bioavailability, *in vitro* and *in vivo* stability, as well as preventing their unwanted interactions with other molecules [6]. They may contain, in addition to phospholipids, other molecules such as cholesterol (Ch) which is an important component of most natural membranes. The incorporation of Ch may increase the stability by modulating the fluidity of the lipid bilayer preventing crystallization of the phospholipid acyl chains and providing steric hindrance to their movement. Further advances in liposome research found that polyethylene glycol (PEG), which is inert in the body, allows longer circulatory life of the drug delivery system [7].

In this work we describe the synthesis of new fluorescent di(hetero)arylethers in the thieno[3,2-*b*]pyridine series, by copper-catalyzed Ullmann-type C-O coupling of the methyl 3-amino-6-bromo-thieno[3,2-*b*]pyridine-2-carboxylate, earlier prepared by us [8], with *o*-, *m*- and *p*-methoxyphenols. The effects of the three coupling products obtained in the growth inhibition of human tumor cell lines, MCF-7 (breast adenocarcinoma), A375-C5 (melanoma), NCI-H460 (non-small cell lung cancer), were evaluated and the *ortho* and *meta*-methoxydi(hetero)arylethers were shown to be the most promising antitumor compounds, presenting very low GI_{50} values in all the cell lines studied. For the latter compounds, the fluorescence properties were evaluated in different solvents and when encapsulated in different nanoliposome formulations, with or without cholesterol and PEG. Fluorescence anisotropy measurements can give relevant information about the compound behavior and location in the several liposomes, namely if they are located in the lipid bilayer, feeling the differences between the gel and the liquid-crystalline phases of phospholipids. These studies are important keeping in mind future drug delivery applications of these new potential anticancer drugs.

2. Experimental

2.1. Synthesis

2.1.1.General Remarks

Melting points (^{o}C) were determined in a SMP3 Stuart apparatus and are uncorrected. ^{1}H and ^{13}C NMR spectra were recorded on a Bruker Avance III at 400 and 100.6 MHz, respectively. Heteronuclear correlations, ^{1}H-^{13}C, HMQC or HSQC were performed to attribute some signals.

MS and HRMS data were recorded using a method of direct injection by EI (70eV) and by the mass spectrometry service of the University of Vigo, Spain.

The reactions were monitored by thin layer chromathography (TLC) in aluminium plates covered with a layer of silica gel 60 (*Macherey-Nagel*) of 0.2 mm, with UV_{254} fluorescence indicator. Column chromatography was performed on Macherey-Nagel silica gel 230-400 mesh, using a solvent gradient, increasing the polarity in mixtures of diethylether/ petroleum ether in portions of 10% of diethylether until product isolation. Petroleum ether refers to the boiling range 40-60 ^{o}C.

*2.1.2. General procedure for the copper-catalyzed C-O (Scheme 1)***:** In a Schlenk tube, dry dioxane (3 mL), CuI (10 mol%), *N*,*N*-dimethylglycine (30 mol%), the corresponding phenol (1.3 equiv.), Cs_2CO_3 (2.0 equiv.) and methyl 3-amino-6-bromothieno[3,2-*b*]pyridine-2-carboxylate (**1**), were added under argon, and the mixture was heated with stirring at 110 ^{o}C for 8 hours. After cooling, NaOH aqueous (30% w/v) and ethyl acetate were added. The phases were separated, the organic phase was dried ($MgSO_4$) and filtered. The solvent was evaporated under reduced pressure giving a solid which was submitted to column chromatography.

2.1.2.1. Methyl 6-(2-methoxyphenoxy)-3-aminothien[3,2-*b*]pyridine-2-carboxylate (**2a**)**:** Thieno[3,2-*b*]pyridine **1** (150 mg, 0.545 mmol) and 2-methoxyphenol (1.3 equiv, 0.1 mL, 0.709 mmol), were heated and the reaction mixture was treated according to the general procedure. Column chromatography using 60% diethylether/petroleum ether gave compound **2a** as a yellow solid (67.0 mg, 40%), m.p. 137-139 ^{o}C, after some washes with petroleum ether. ^{1}H NMR ($CDCl_3$, 400 MHz): δ 3.81 (3H, s, OMe), 3.89 (3H, s, OMe), 6.21 (2H, s largo, NH_2), 6.99-7.01 (1H, m, Ar-H), 7.06 (1H, dd, *J* = 8.4 e 1.6 Hz, ArH), 7.12 (1H, dd, *J* = 8.0 e 1.6 Hz, ArH), 7.24-7.38 (1H, m, Ar-H), 7.34 (1H, d, *J* = 2.4 Hz, HetAr), 8.46 (1H, d, *J* = 2.4 Hz, HetAr) ppm. ^{13}C NMR ($CDCl_3$, 100.6 MHz): δ 51.55 (OMe), 55.85 (OMe), 98.17 (C),

113.07 (CH), 116.11 (CH), 121.41 (CH), 122.07 (CH), 126.49 (CH), 135.33 (C), 138.54 (CH), 141.22 (C), 143.15 (C), 147.38 (C), 151.45 (C), 154.46 (C), 165.30 (C=O) ppm. MS (EI) m/z (%): 330.07 (M^+,100), 298.04 (M^+-OMe, 69). HRMS M^+ calcd. for $C_{16}H_{14}N_2O_4S$: 330.0674, found 330.0680**.**

2.1.2.2. Methyl 6-(3-methoxyphenoxy)-3-aminothieno[3,2-*b*]pyridine-2-carboxylate (**2b**)**:** Thieno[3,2-*b*]pyridine **1** (150 mg, 0.545 mmol) and 3-methoxyphenol (1.3 equiv, 0.1 mL, 0.709 mmol), were heated and the reaction mixture was treated according to the general procedure. Column chromatography using 40% diethylether/petroleum ether gave compound **2b** as a yellow solid (96.0 mg, 53%), m.p. 111-112 ^oC, after some washes with petroleum ether. ^1H NMR ($CDCl_3$, 400 MHz): δ 3.81 (3H, s, OMe), 3.90 (3H, s, OMe), 6.21 (2H, s largo, NH_2), 6.63-6.66 (2H, m, ArH), 6.74-6.77 (1H, m, ArH), 7.27-7.32 (1H, m, ArH), 7.53 (1H, d, *J* = 2.4 Hz, HetArH), 8.45 (1H, d, *J* = 2.4 Hz, HetAr) ppm. ^{13}C NMR ($CDCl_3$, 100.6 MHz): δ 51.56 (OMe), 55.44 (OMe), 98.60 (C), 105.54 (CH), 110.28 (CH), 111.38 (CH), 118.41 (CH), 130.61 (CH), 135.18 (C), 139.89 (CH), 142.02 (C), 147.34 (C), 153.48 (C), 156.48 (C), 161.23 (C), 165.24 (C=O) ppm. MS (EI) m/z(%): 330.07 (M^+,100), 298.04 (M^+-OMe, 67), HRMS M^+ calcd. for $C_{16}H_{14}N_2O_4S$: 330.0674, found 330.0675.

2.1.2.3. Methyl 6-(4-methoxyphenoxy)-3-aminothieno[3,2-*b*]piridine-2-carboxylate (**2c**)**:** Thieno[3,2-*b*]pyridine **1** (100 mg, 0.363 mmol) and 4-methoxyphenol (1.0 equiv, 44.0 mg, 0,363 mmol), were heated and the reaction mixture was treated according the general procedure. Column chromatography using 50% diethylether/petroleum ether gave compound **2c** as a yellow solid (79.0 mg, 65%), m.p. 129-131 ^oC, after some washes with petroleum ether. ^1H NMR ($CDCl_3$, 400 MHz): δ 3.84 (3H, s, OMe), 3.90 (3H, s, OMe), 6.27 (2H, s largo, NH_2), 6.95 (2H, d, *J* = 9.2 Hz, 2xArH), 7.05 (2H, d, *J* = 9.2 Hz, 2xArH), 7.44 (1H, d, *J* = 2.4 Hz, HetArH), 8.44 (1H, d, *J* = 2.4 Hz, HetArH) ppm. ^{13}C NMR ($CDCl_3$, 100.6 MHz): δ 51.55 (OMe), 55.68 (OMe), 98.29 (C), 115.29 (2×CH), 116.64 (CH), 121.21 (2×CH), 135.29 (C), 139.31 (CH), 141.44 (C), 147.41 (C), 148.65 (C), 154.90 (C), 158.84 (C), 165.30 (C=O) ppm. MS (EI) m/z(%): 330.07 (M^+,100), 298.04 (M^+-OMe, 68), HRMS M^+ calcd. for $C_{16}H_{14}N_2O_4S$: 330.0674, found 330.0671.

2.2. Biological Activity

2.2.1. Reagents

Fetal bovine serum (FBS), L-glutamine, phosphate buffered saline (PBS) and trypsin were from Gibco Invitrogen Co. (Scotland, UK). RPMI-1640 medium was from Cambrex (New Jersey, USA). Acetic acid, dimethyl sulfoxide (DMSO), doxorubicin, penicillin, streptomycin, ethylenediaminetetraacetic acid (EDTA), sulforhodamine B (SRB) and trypan blue were from SigmaChemical Co. (Saint Louis, USA). Tricloroacetic acid (TCA) and Tris were sourced from Merck (Darmstadt, Germany).

2.2.2. Solutions of the compounds

Stock solutions of the tested compounds were prepared in DMSO and kept at −70°C. Appropriate dilutions were freshly prepared in the test medium just prior to the assays. The effect of the vehicle solvent (DMSO) on the growth of the cell lines was evaluated by exposing untreated control cells to the maximum concentration of DMSO used in the assays (0.25%). No influence was found (data not shown).

2.2.3. Cell cultures

Three human tumor cell lines, MCF-7 (breast adenocarcinoma), NCI-H460 (non-small cell lung cancer) and A375-C5 (melanoma) were used. MCF-7 and A375-C5 were obtained from the European Collection of Cell Cultures (ECACC, Salisbury, UK), and NCI-H460 was kindly provided by the National Cancer Institute (NCI, Bethesda, USA). They were routinely maintained as adherent cell cultures in RPMI-1640 medium supplemented with 5% heat-inactivated FBS, 2 mM glutamine and antibiotics (penicillin 100 U/mL, streptomycin 100 μg/mL), at 37°C in a humidified atmosphere containing 5% CO_2. Exponentially growing cells were obtained by plating 1.5×10^5 cells/mL for MCF-7 and 0.75×10^5 cells/mL for A375-C5 and NCI-H460, followed by a 24 h incubation.

2.2.4. Cell growth inhibition assay

The effects on the *in vitro* growth of human tumor cell lines were evaluated according to the procedure adopted by the NCI (USA) in their "*In vitro* Anticancer Drug Discovery Screen", using the protein-binding dye sulforhodamine B to assess cell growth [9,10]. Briefly, exponentially growing cells were exposed for 48 h, in 96-well microtiter plates, to five serial dilutions of each test compound, starting from a maximum concentration of 150 μM (if possible). Following the exposure period adherent cells were fixed *in situ*, washed and stained

with SRB. The bound stain was solubilized and the absorbance was measured at 492 nm in a plate reader (Biotek Instruments Inc., Powerwave XS, Wincoski, USA). Dose-response curves were obtained for each test compound and cell line, and the growth inhibition of 50% (GI_{50}), corresponding to the concentration of the compounds that inhibited 50% of the net cell growth was calculated as described elsewhere [10]. Doxorubicin was tested in the same manner to be used as a positive control.

2.3. Liposomes preparation

All the solutions were prepared using spectroscopic grade solvents and ultrapure water (Milli-Q grade). 1,2-Dipalmitoyl-*sn*-glycero-3-phosphocholine (DPPC), 1,2-distearoyl-*sn*-glycero-3-phosphocholine (DSPC), 1,2-diacyl-*sn*-glycero-3-phosphocholine from egg yolk (egg-PC), 1,2-dimyristoyl-*sn*-glycero-3-[phospho-*rac*-(1-glycerol)] (sodium salt) (DMPG) and cholesterol (Ch) were obtained from Sigma-Aldrich. 1,2-Distearoyl-*sn*-glycero-3-phosphoethanolamine-*N*-[methoxy(poly-ethylene glycol)-2000] (ammonium salt) (DSPE-PEG) was obtained from Avanti Polar Lipids, while dioctadecyldimethylammonium bromide (DODAB) was from Tokyo Kasei (lipid structures are shown below).

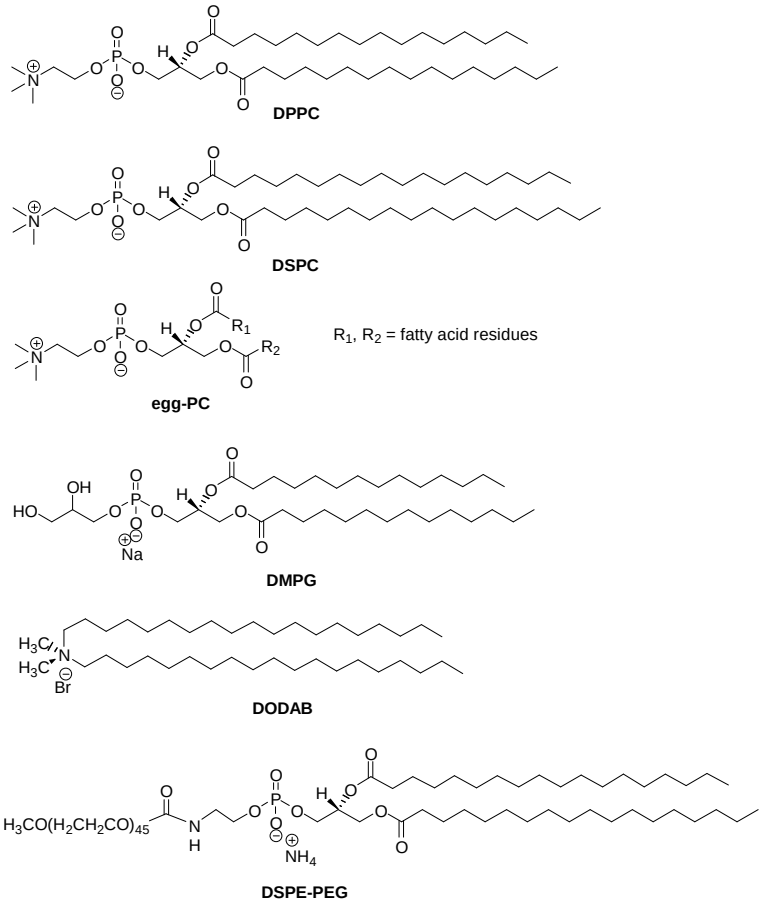

Nanoliposomes were prepared by evaporation of a mixture of lipids and compound in chloroform under vacuum for 12 h. The lipid/compound film was then hydrated with an aqueous buffer solution (10 mM Tris-HCl buffer, pH=7.4), above the lipids melting transition temperature (*ca.* 41 ºC for DPPC [11], 23 ºC for DMPG [12], 55 ºC for DSPC [13] and 45 ºC for DODAB [14]), followed by six extrusion cycles (using a LIPEX^{TM} extruder) through 100 nm polycarbonate membranes. Between the extrusion cycles, the solutions were allowed to equilibrate for 1 h. The final total lipid concentration was 1 mM, with a compound/lipid molar ratio of 1:333.

DLS and zeta potential measurements: Liposomes mean diameter and size distribution (polydispersity index) were measured using a Dynamic Light Scattering (DLS) equipment (NANO ZS Malvern Zetasizer), at 25 ºC, using a He-Ne laser of 633 nm and a detector angle of 173º. Five independent measurements were performed for each sample. Malvern Dispersion Technology Software (DTS) was used with multiple narrow mode (high resolution) data processing, and mean size (nm) and error values were considered.

2.4. Spectroscopic measurements

Absorption spectra were recorded in a Shimadzu UV-3101PC UV-Vis-NIR spectrophotometer. Fluorescence measurements were performed using a Fluorolog 3 spectrofluorimeter, equipped with double monochromators in both excitation and emission, Glan-Thompson polarizers and a temperature controlled cuvette holder. Fluorescence spectra were corrected for the instrumental response of the system.

For fluorescence quantum yield determination, the solutions were previously bubbled for 20 minutes with ultrapure nitrogen. The fluorescence quantum yields (Φ_s) were determined using the standard method (equation 1) [15,16]. Quinine sulfate in H_2SO_4 0.05 M was used as reference, $\Phi_r = 0.546$ at 25 ºC [17].

$$\Phi_s = \left[\left(A_r F_s n_s^2\right)/\left(A_s F_r n_r^2\right)\right]\Phi_r \qquad (1)$$

where *A* is the absorbance at the excitation wavelength, *F* the integrated emission area and *n* the refraction index of the solvents used. Subscripts refer to the reference (r) or sample (s) compound. The absorbance value at excitation wavelength was always less than 0.1, in order to avoid inner filter effects.

Solvatochromic shifts can be described by the Lippert-Mataga equation (2), which relates the energy difference between absorption and emission maxima to the orientation polarizability, [18,19]

$$\bar{\nu}_{abs} - \bar{\nu}_{fl} = \frac{1}{4\pi\varepsilon_0} \frac{2\Delta\mu^2}{hcR^3} \Delta f + const \qquad (2)$$

where $\bar{\nu}_{abs}$ is the wavenumber of maximum absorption, $\bar{\nu}_{fl}$ is the wavenumber of maximum emission, $\Delta\mu = \mu_e - \mu_g$ is the difference in the dipole moment of solute molecule between excited (μ_e) and ground (μ_g) states, R is the cavity radius (considering the fluorophore a point dipole at the center of a spherical cavity immersed in the homogeneous solvent), and Δf is the orientation polarizability given by (eq. 3):

$$\Delta f = \frac{\varepsilon - 1}{2\varepsilon + 1} - \frac{n^2 - 1}{2n^2 + 1} \quad , \qquad (3)$$

where ε is the static dielectric constant and n the refractive index of the solvent.

An alternative expression, proposed by Bakhshiev, takes into account the angle, γ, between the ground and excited state dipole moments of the fluorophore [20,21]:

$$\bar{\nu}_{abs} - \bar{\nu}_{fl} = \frac{1}{4\pi\varepsilon_0} \frac{2}{hcR^3} \left(\mu_g^2 - 2\mu_g\mu_e \cos\gamma + \mu_e^2\right) f(\varepsilon, n) + const \qquad (4)$$

where $\mu_g^2 - 2\mu_g\mu_e \cos\gamma + \mu_e^2$ is equivalent to $\left|\vec{\mu}_e - \vec{\mu}_g\right|^2$ and

$$f(\varepsilon, n) = \frac{\varepsilon - 1}{\varepsilon + 2} - \frac{n^2 - 1}{n^2 + 2} \qquad (5)$$

The steady-state fluorescence anisotropy, r, is calculated by

$$r = \frac{I_{VV} - G\, I_{VH}}{I_{VV} + 2G\, I_{VH}} \qquad (6)$$

where I_{VV} and I_{VH} are the intensities of the emission spectra obtained with vertical and horizontal polarization, respectively (for vertically polarized excitation light), and $G = I_{HV}/I_{HH}$ is the instrument correction factor, where I_{HV} and I_{HH} are the emission intensities obtained with vertical and horizontal polarization (for horizontally polarized excitation light).

3. Results and discussion

3.1. Synthesis

New di(heteroaryl)ethers **2a-c** were prepared by copper-catalyzed C-O coupling of the methyl 3-amino-6-bromothieno[3,2-*b*]pyridine-2-carboxylate (**1**), earlier prepared by us [8], with *ortho*, *meta* and *para*-methoxyphenols, using CuI as the catalyst, *N*,*N*-dimethylglycine as the ligand and Cs_2CO_3 as the base, in moderate to good yields (Scheme 1).

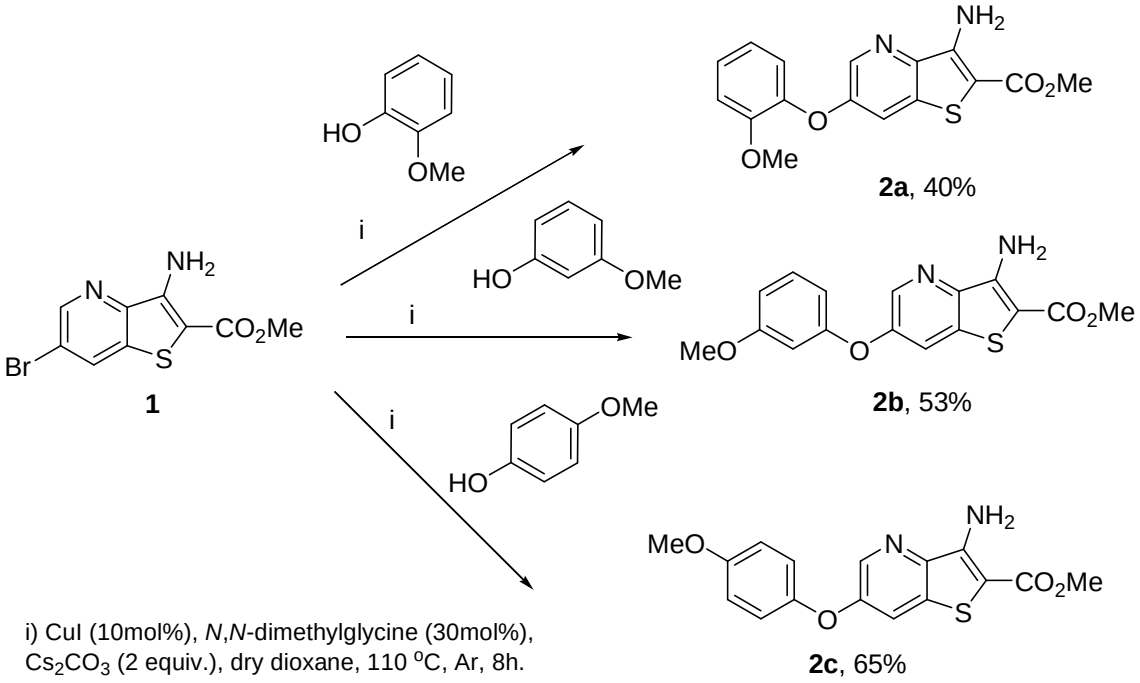

Scheme 1. Synthesis of di(hetero)arylethers **2a-c** by copper-catalyzed C-O coupling

The Ullmann ether synthesis has been extensively used for the formation of diarylethers [22,23]. However, the harsh reaction conditions (125-220 ^{o}C in neat phenol or solvents such as pyridine collidine or *N*,*N*-dimethylformamide), the usual requirement for stoichiometric (or higher) quantities of copper, and the fact that unactivated aryl halides usually react in low yields have limited the utility of this reaction [22]. Thus, development of methods for the synthesis of diarylethers under relatively mild conditions is receiving increasing interest. Ma and Cai reported for the first time in 2003 that, under the action of *N*,*N*-dimethylglycine as the ligand, CuI-catalyzed coupling reaction of aryl halides and phenols using Cs_2CO_3 as the base, could be carried out at 90 ^{o}C to give the corresponding diarylethers [24]. As described for the amino acid promoted CuI-catalyzed C-N bond formation from aryl halides and amines or *N*-containing heterocycles, the mechanism for the formation of the diarylethers (C-O bond formation) may occur through two pathways:1) oxidative addition/reductive elimination; 2) π-

complex mechanism. Based on the fact that copper ions can form chelates with amino acids through the carboxyl and amino groups, Ma *et al.* put forward two possible catalytic cycles [25].

3.2. Biological activity

The effects of the di(hetero)arylethers **2a-c** on the human tumor cells growth were evaluated in three human tumor cell lines MCF-7 (breast adenocarcinoma), A375-C5 (melanoma), NCI-H460 (non-small cell lung cancer) and the results are presented in Table 1. The di(hetero)arylethers bearing a methoxy group in the *ortho* and *meta* positions **2a** and **2b**, respectively, are the most promising antitumor compounds presenting very low GI_{50} values (1.1-2.5 μM) in the tumor cell lines in study. The position of the methoxy group is very important for the activity, since compound **2c** with the methoxy group in the *para* position relative to the ether function, presented very much higher GI_{50} values.

Doxorubicin, used as positive control, presents very high citotoxicity in these cell lines but it is also very toxic for the human body and nowadays is used in a liposomal pegylated formulation that decreases their toxicity and adverse secundary effects and increases the captation by the tumor [26-28].

Table 1. Growth inhibitory activity of the di(hetero)arylethers **2a-c** on the three human tumor cell lines in study.

Compounds	**GI_{50} (μM) [a]**		
	MCF-7	**A375-C5**	**NCI-H460**
2a	1.4 ± 0.1	1.4 ± 0.1	1.1 ± 0.1
2b	2.5 ± 0.1	2.5 ± 0.3	2.3 ± 0.1
2c	46.8 ± 4.0	83.5 ± 5.8	45.0 ± 1.4

[a] The lowest concentrations causing 50% of cell growth inhibition (GI_{50}) after a continuous exposure of 48 h, expressed as means ± SEM of three independent experiments performed in duplicate. Doxorubicin was used as positive control (GI50: MCF-7 = 43.3 ± 2.6 nM; A375-C5 = 130.2 ± 10.1 nM; NCI-H460 = 35.6 ± 1.6 nM).

Due to the antitumoral potential of the di(hetero)arylethers **2a**–**b** and as both are fluorescent, their photophysical properties were studied. Also, their encapsulation in nanoliposomes for future drug delivery purposes was monitored using the intrinsic fluorescence of the compounds.

3.3. Fluorescence studies in several solvents

The absorption and fluorescence properties of compounds **2a** and **2b** were studied in several solvents (Table 2). The normalized fluorescence spectra of both compounds are shown in Figures 1 and 2, respectively. Examples of absorption spectra are shown as insets.

Compounds **2a** and **2b** exhibit reasonable fluorescence in several solvents. Fluorescence quantum yield values are in the range of 3% in chloroform and 34% in DMSO for compound **2a** and of 2% (chloroform) and 29% (DMSO) for compound **2b** (Table 2). However, no emission is observed in protic solvents, like water or ethanol. This behaviour can be due to specific solute-solvent interactions by hydrogen bonds with protic solvents, namely by protonation of the N atom of the pyridine ring. The same explanation can justify the low fluorescence quantum yields obtained in chloroform, as the formation of hydrogen bonds between chloroform and proton acceptor molecules is known since a long time [29].

Table 2. Maximum absorption (λ_{abs}) and emission wavelengths (λ_{em}), molar absorption coefficients (ε) and fluorescence quantum yields (Φ_F) for compounds **2a** and **2b** in several solvents.

Solvent	**λ_{abs} (nm) (ε/10^4 M^{-1} cm^{-1})**		**λ_{em} (nm)**		**Φ_F [a]**	
	2a	**2b**	**2a**	**2b**	**2a**	**2b**
Cyclohexane	359 (0.37), 310 (0.54), 288 (3.07)	360 (0.39), 311 (0.61), 289 (3.06)	425	427	0.26	0.29
Dioxane	360 (0.55); 289 (3.69)	361 (0.46), 289 (3.00)	440	441	0.27	0.28
Ethyl acetate [b]	355 (0.50), 309 (0.77), 287 (3.40)	361 (0.45), 312 (0.71) 288 (3.02)	448	453	0.07	0.09
Dichloromethane	354 (0.58), 310 (0.89), 288 (3.49)	355 (0.45), 311 (0.69), 288 (2.80)	447	451	0.13	0.16
N,*N*-Dimethylformamide [b]	358 (0.56), 289 (3.39)	357 (0.59), 290 (3.02)	465	470	0.20	0.12
Dimethylsulfoxide [b]	362 (0.62), 290 (3.42)	364 (0.47), 291 (2.71)	475	479	0.34	0.29
Acetonitrile	354 (0.55), 309 (0.84), 286 (3.46)	355 (0.38), 310 (0.60), 287 (2.48)	459	461	0.14	0.12
Chloroform [b]	354 (0.57), 311 (0.91), 289 (3.50)	361 (0.46), 313 (0.87) 290 (2.88)	445	448	0.03	0.02
Ethanol	359 (0.56), 310 (0.88), 288 (3.72)	361 (0.41), 311 (0.77), 289 (2.83)	---	---	---	---
Methanol	358 (0.56), 310 (0.89), 287 (3.69)	361 (0.46); 288 (3.06)	---	---	---	---

[a] Relative to quinine sulfate in H_2SO_4 0.05 M (Φ_F = 0.546 at 25 ºC [16]). Error about 10%.

[b] *Solvents cut-off*: Dimethylsulfoxide: 270 nm; *N*,*N*-Dimethylformamide: 275 nm; Ethyl acetate: 265 nm; Chloroform: 250 nm.

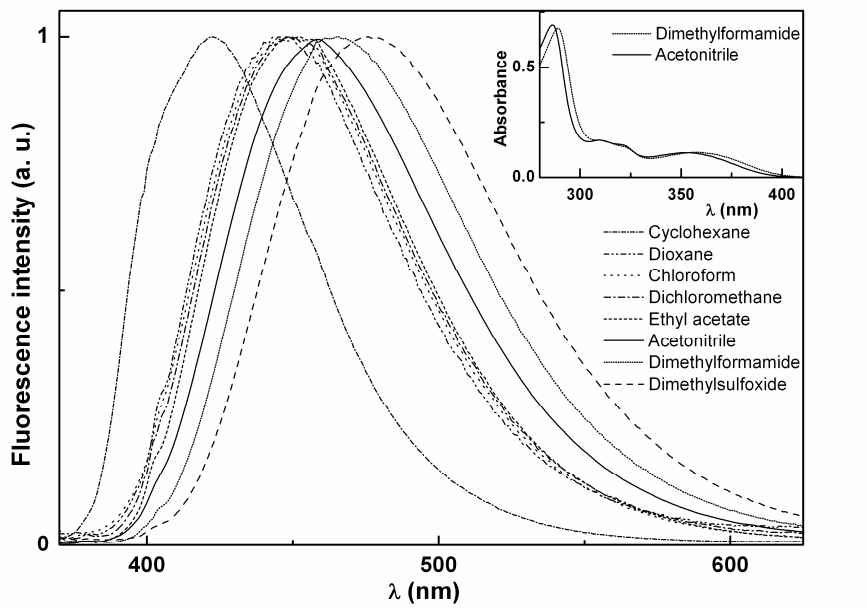

Figure 1. Normalized fluorescence spectra of 3×10^{-6} M solutions of compound **2a** in several solvents (λ_{exc}=360 nm). Inset: Absorption spectrum of 2×10^{-5} M solutions of **2a** in acetonitrile and dimethylformamide, as examples.

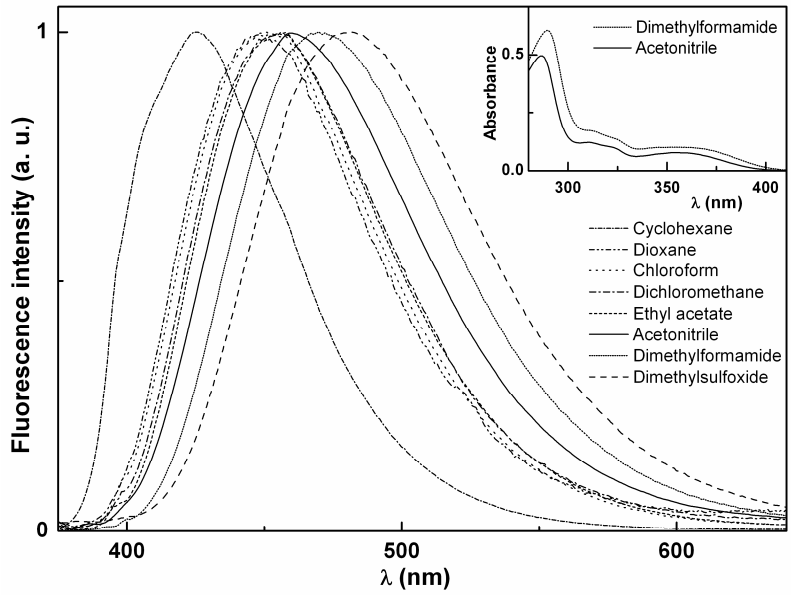

Figure 2. Normalized fluorescence spectra of 3×10^{-6} M solutions of compound **2b** in several solvents (λ_{exc}=355 nm). Inset: Absorption spectrum of 2×10^{-5} M solutions of **2b** in acetonitrile and dimethylformamide, as examples.

For both compounds, significant red shifts are observed for emission in polar solvents (50 nm between cyclohexane and dimethylsulfoxide for compound **2a** and 52 nm for **2b**). In the absorption spectra, the red shifts are negligible (Table 2), indicating that solvent relaxation after photoexcitation plays an important role. In polar solvents, a clear band enlargement in

emission is also observed (Figs. 1 and 2), which is usually related to an intramolecular charge transfer (ICT) mechanism and/or to specific solvent effects [18].

The solvatochromic plots for compounds **2a**–**b**, shown in Figure 3, are reasonably linear, the slope being larger for compound **2b**. This shows that the presence of the methoxy group in the *meta* position causes an enhance of the ICT character of the excited state.

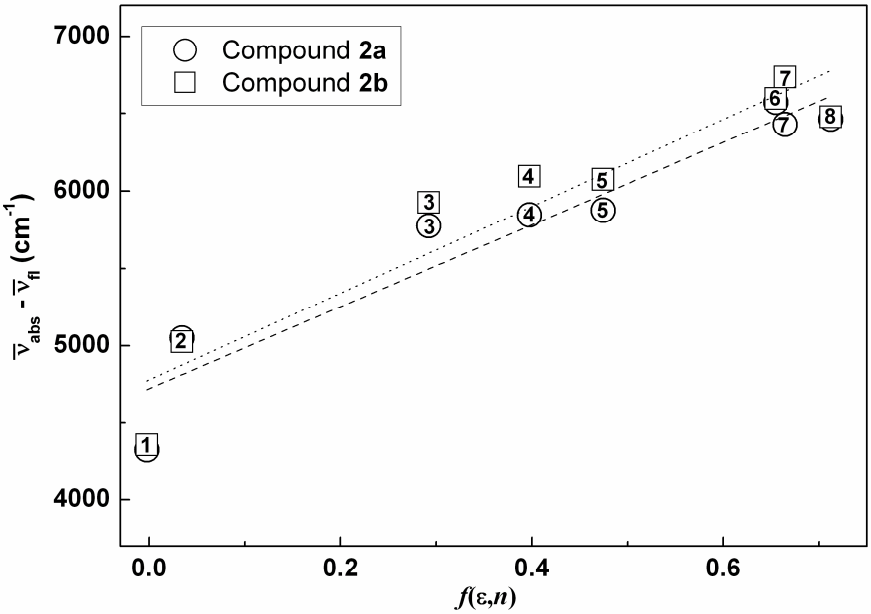

Figure 3. Solvatochromic plots (equation 4) for compounds **2a** and **2b**. Solvents: 1 - cyclohexane; 2 - dioxane; 3 - chloroform; 4 - ethyl acetate; 5 - dichloromethane; 6 - dimethylsulfoxide; 7 - *N*,*N*-dimethylformamide; 8 - acetonitrile (values of ε and *n* were obtained from ref. [30]).

From *ab initio* molecular quantum chemistry calculations, obtained with Gaussian 09 software [31] and use of a 6-311+G(dp) basis set at the TD-SCF DFT (B3LYP) level of theory [32] in gas phase, the cavity radius (*R*) and the ground state dipole moment (μ_g) were determined for the two compounds (Table 3). The optimized geometry of the ground state of the di(hetero)arylethers **2a-b** shows that the methoxyphenyl moiety is completely out of the plane of the thienopyridine system. In the lowest excited state a distortion occurs, which is much more pronounced in compound **2b**, where the two moieties are further apart (Figure 4). The directions of the calculated dipole moments in the ground and excited state are also indicated in Figure 4, evidencing a change in the excited state dipole moment vector to almost the opposite direction relative to the ground state one. This clearly indicates that the angle between the two dipole moment vectors cannot be neglected and must be considered in the solvatochromic plots (Bakhshiev's equation (4)).

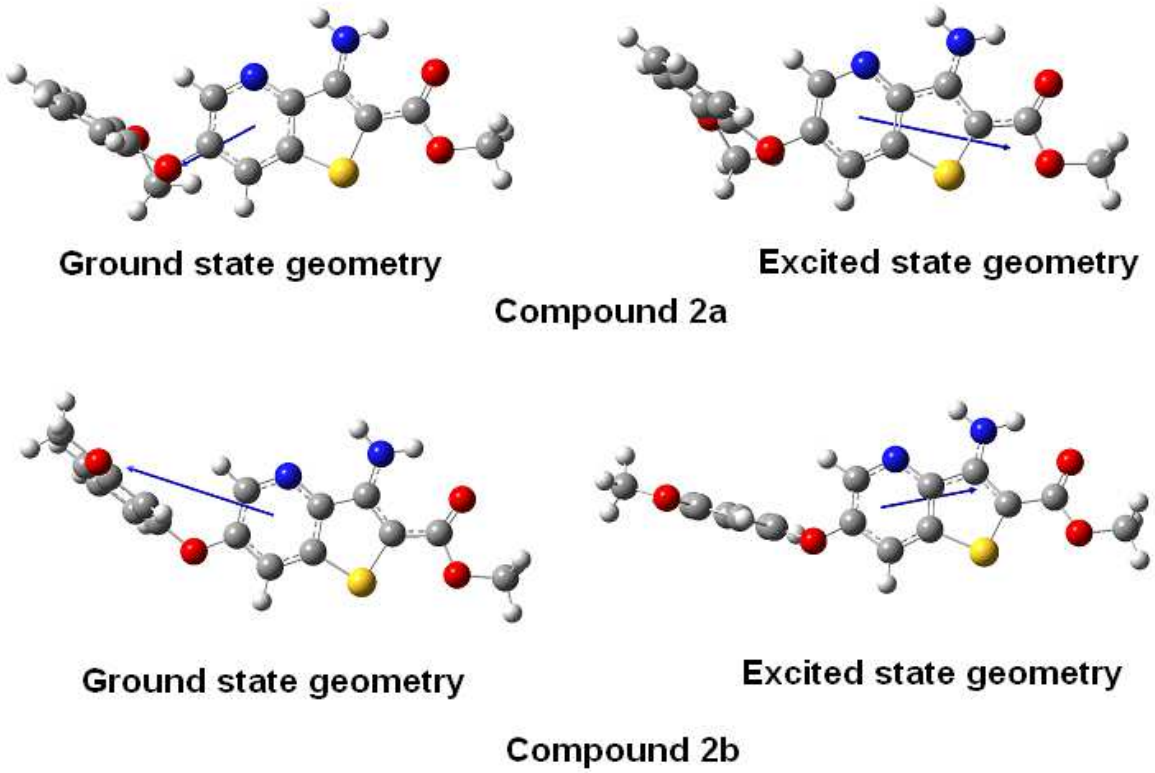

Figure 4. Optimized geometries of compounds **2a** and **2b** obtained by Gaussian 09 software (grey: C atoms; white: H atoms; red: O atoms; blue: N atoms; yellow: S atoms). Left: ground state; Right: lowest excited singlet state. The arrows indicate the direction of the dipole moment.

The absolute value of the difference in the excited and ground state dipole moment vectors, estimated from the solvatochromic plots (Figure 3) and from molecular quantum mechanical calculations, are presented in Table 3. The obtained values are similar and, therefore, both methods point to the presence of a significant charge transfer mechanism in the excited state, more pronounced for compound **2b**.

Table 3. Cavity radius (R), ground (μ_g) and excited state (μ_e) dipole moments obtained from theoretical calculations, and absolute value of the dipole moment difference ($\left|\vec{\mu}_e - \vec{\mu}_g\right|$), from quantum mechanical calculations and from the solvatochromic plots.

Compound	Cavity radius, R (Å)	Ground state dipole moment, μ_g (D)	Excited state dipole moment, μ_e (D), from theoretical calculations	$\left\|\vec{\mu}_e - \vec{\mu}_g\right\|$ (D) from theoretical calculations	$\left\|\vec{\mu}_e - \vec{\mu}_g\right\|$ (D) from solvatochromic plots
2a	5.4	2.8	4.7	7.1	6.5
2b	5.8	4.7	3.4	7.7	7.2

Figure 5 displays the representation of HOMO and LUMO molecular orbitals for the two compounds, obtained with the calculated optimized geometries for the ground and the lowest excited singlet state. It can be observed that the HOMO and LUMO molecular orbitals are mainly located in the thieno[3,2-*b*]pyridine system, with a small contribution of the ether oxygen atom. The HOMO-LUMO transition (for both geometries) of these compounds shows a significant charge transfer from the amine group linked to the thiophene ring and from its S atom to the pyridine moiety. A charge density decrease in the oxygen atom of the carbonyl group is also observed in the HOMO-LUMO transition. This confirms the CT character of the excited state for both compounds.

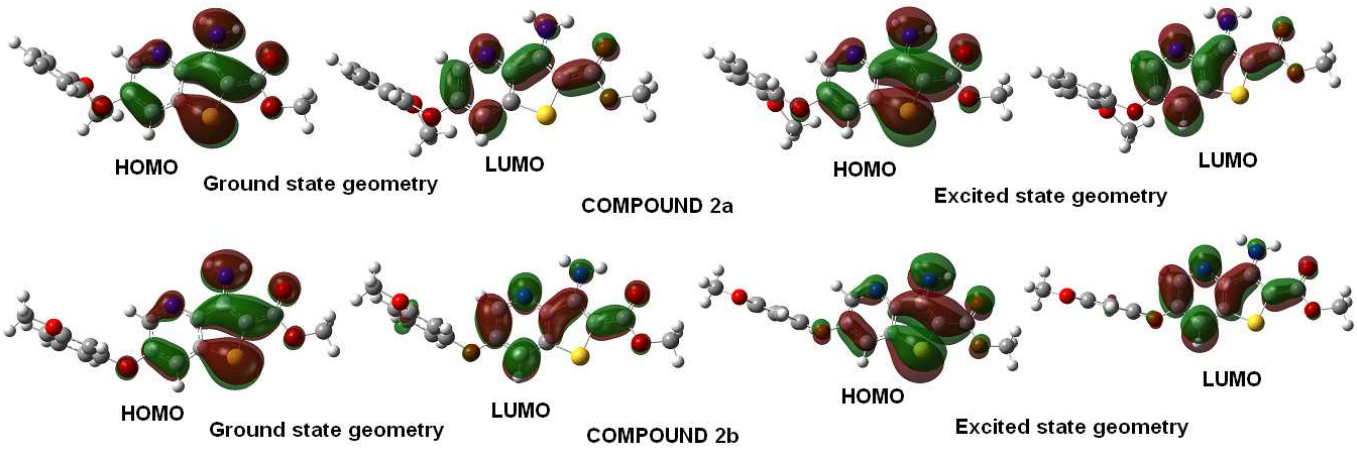

Figure 5. Representation of HOMO and LUMO molecular orbitals of the di(hetero)arylethers **2a** (above) and **2b** (below). Left: Optimized geometry for the ground state; Right: Optimized geometry for the lowest excited singlet state.

The photophysical behavior of both compounds shows that they can be considered as solvatochromic probes. The significant sensitivity of the fluorescence emission to the fluorophore environment can be very useful when probing the location/behavior of these compounds in liposomes.

3.4. Fluorescence studies in nanoliposomes

Fluorescence experiments of both compounds encapsulated in liposomes of several compositions were carried out. These liposomes were composed either by neat phospholipids, or by phospholipid mixtures, with or without cholesterol (Ch) and PEG. Several different lipid compositions were studied, keeping in mind future drug delivery applications of **2a** and **2b** as potential anticancer drugs.

First, liposomes of neat DPPC (zwitterionic), DMPG (anionic), DODAB (cationic) and Egg-PC (zwitterionic, composed of a phosphatidyl choline mixture) with encapsulated compounds were prepared and fluorescence emission was monitored in both gel (below the melting temperature, T_m) and liquid-crystalline (above T_m) phases of the lipid. At room temperature, the phospholipids DPPC and DODAB are in ordered gel phase, where the hydrocarbon chains are fully extended and closely packed. DMPG has a melting transition temperature very near room temperature (T_m = 23 ºC). The melting transition temperature of Egg-PC is very low [33] and this lipid is in the fluid liquid-crystalline phase at room temperature. Fluorescence spectra of compounds **2a-b** incorporated in these liposomes are presented in Figure 6. The maximum emission wavelengths in Egg-PC and DPPC lipid membranes point to a hydrophobic environment for both compounds in lipid membranes (Figure 6, Table 4). In DODAB and DMPG aggregates, a band enlargement and a shift to higher emission wavelengths is observed, indicating a more hydrated environment for the compounds in these aggregates. The red shift is more significant for both compounds in DMPG aggregates, which can be explained by the formation of DMPG unilamellar vesicles with perforations [34], or leaky vesicles [35], where the compounds may feel more penetration of water molecules.

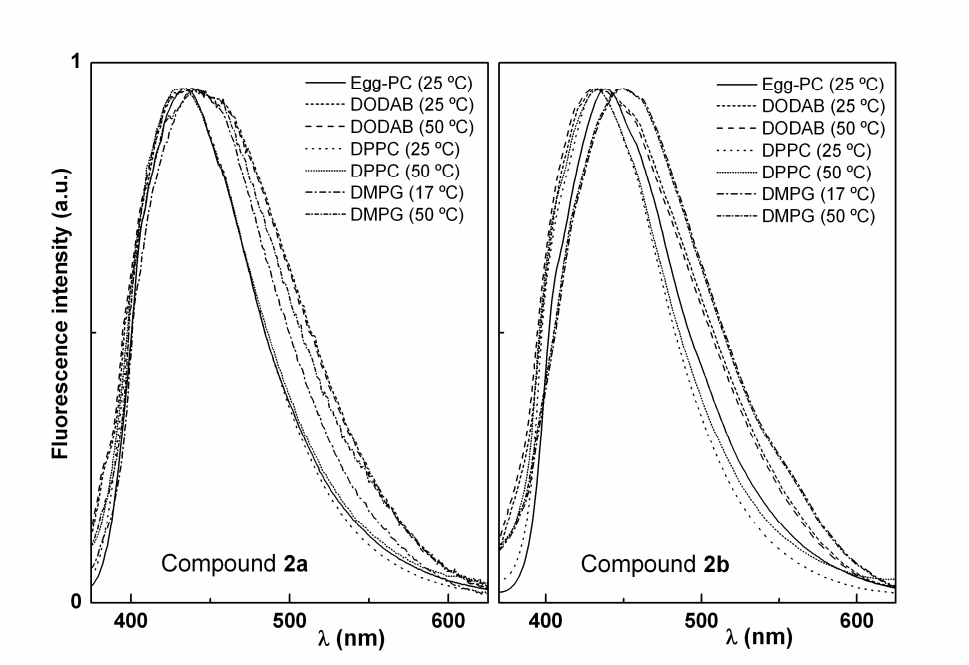

Figure 6. Normalized fluorescence spectra of compounds **2a** and **2b** (3×10^{-6} M) in lipid aggregates of Egg-PC, DPPC, DMPG and DODAB, below (17 ºC or 25 ºC) and above (50 ºC) the melting temperature of the lipids.

Table 4. Steady-state fluorescence anisotropy (*r*) values and maximum emission wavelengths (λ_{em}) for compounds **2a** and **2b** in lipid aggregates, below (17 ºC or 25 ºC) and above (50 ºC) transition temperature of the lipids. Anisotropy values in glycerol at room temperature are also shown for comparison.

Lipid	T (º C)	Compound **2a**		Compound **2b**	
		λ_{em} (nm)	***r***	**λ_{em} (nm)**	***r***
Egg-PC	25	433	0.121	436	0.120
DPPC	25	432	0.196	433	0.186
	50	432	0.095	434	0.075
DODAB	25	439	0.179	437	0.155
	50	438	0.115	436	0.112
DMPG	17	443	0.147	447	0.154
	50	442	0.105	446	0.108
Glycerol	25	420	0.295	418	0.309

Fluorescence anisotropy (*r*) measurements (Table 4) can give relevant information about the location of the compounds in liposomes, as *r* increases with the rotational correlation time of the fluorescent molecule (and, thus, with the viscosity of the fluorophore environment) [36]. Anisotropy values in a viscous solvent (glycerol) were also determined, for comparison. Steady-state fluorescence anisotropy results (Table 4) allow concluding that both compounds are mainly located in the inner region of the lipid membrane, feeling the penetration of water molecules, especially in DMPG aggregates. The transition from the rigid gel phase to the fluid liquid-crystalline phase is clearly detected by a notable decrease in anisotropy at 50 ºC. The *r* values in Egg-PC liposomes at 25 ºC (fluid phase) are also significantly lower than those observed in lipids which are in the gel phase at this temperature.

Considering future developments of these compounds delivery using nanoliposomes as drug carriers, several different liposome formulations were prepared [37-39], some of them containing cholesterol (Ch) and polyethylene glycol (PEG). The incorporation of Ch may increase the stability by modulating the fluidity of the lipid bilayer, preventing crystallization of the phospholipid acyl chains and providing steric hindrance to their movement. Further advances in liposome research found that PEG, which is inert in the body, allows longer circulatory life of the drug delivery system [7].

Previous studies have shown that DODAB-based liposomes exhibit very large sizes (diameter larger than 250 nm) [39-41] and, for this reason, this cationic lipid was not used in the liposome formulations prepared. On the contrary, most of the nanoliposomes contain DMPG, as the presence of pores across this lipid membrane has a promising biological relevance in applications for controlled release from nanocompartments [34].

The size and size distribution (polydispersity index) of the prepared nanoliposomes with encapsulated compounds **2a** and **2b** were obtained by DLS. All the liposomes have a mean hydrodynamic diameter lower than 140 nm and generally low polydispersity (Table 5). The Egg-PC:Ch (7:3), Egg-PC:Ch:DMPG (7:3:1) and DSPC:Ch:DSPE-PEG_{2000} (1:1:0.75) formulations allowed us to obtain the smaller nanoliposome diameters, which are lower than 100 nm for both compounds. The Egg-PC:Ch formulation is the one with a lower polydispersity.

Table 5. Mean hydrodynamic diameter and polydispersity of several nanoliposome formulations with encapsulated compounds **2a** and **2b**, at 25 ºC.

Formulation	Compound **2a**		Compound **2b**	
	Hydrodynamic diameter (nm) (mean ± SD)	**Polydispersity (mean ± SD)**	**Hydrodynamic diameter (nm) (mean ± SD)**	**Polydispersity (mean ± SD)**
Egg-PC:Ch (7:3)	84.4 ± 0.4	0.19 ± 0.01	87.8 ± 0.4	0.21 ± 0.01
Egg-PC:Ch:DMPG (7:3:1)	81.2 ± 0.5	0.26 ± 0.01	90.2 ± 0.5	0.36 ± 0.02
DPPC:DMPG (1:1)	133.4 ± 0.6	0.34 ± 0.01	116.2 ± 0.6	0.42 ± 0.02
DPPC:DMPG (1:2)	131.7 ± 0.6	0.43 ± 0.02	141.0 ± 0.4	0.24 ± 0.01
DPPC:DMPG (2:1)	125.6 ± 0.5	0.39 ± 0.02	114.1 ± 0.4	0.34 ± 0.01
DSPC:DMPG (5:1)	117.4 ± 0.5	0.34 ± 0.01	136.3 ± 0.6	0.35 ± 0.01
DSPC:Ch:DSPE-PEG_{2000} (1:1:0.75)	83.6 ± 0.4	0.31 ± 0.01	71.7 ± 0.3	0.28 ± 0.01

Standard deviations (SD) were calculated from the mean of the data of a series of five experiments conducted using the same parameters.

The two compounds show significant fluorescence emission when incorporated in nanoliposomes (Figure 7) and steady-state fluorescence anisotropy values are generally high at room temperature (Table 6).

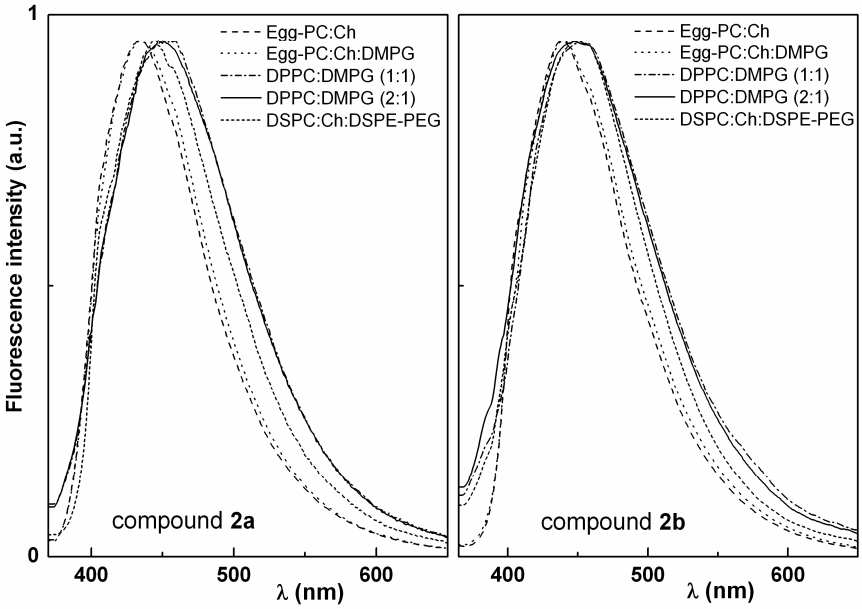

Figure 7. Normalized fluorescence spectra of compounds **2a** and **2b** (3×10^{-6} M) in nanoliposomes of different compositions at room temperature.

Table 6. Steady-state fluorescence anisotropy (*r*) values and maximum emission wavelengths (λ_{em}) for compounds **2a** and **2b** encapsulated in nanoliposomes, at 25 ºC and 50 ºC.

Formulation		Compound **2a**		Compound **2b**	
		λ_{em} (nm)	***r***	**λ_{em} (nm)**	***r***
Egg-PC:Ch (7:3)	25	435	0.117	439	0.109
Egg-PC:Ch:DMPG (7:3:1)	25	434	0.176	441	0.149
	50	433	0.121	442	0.109
DPPC:DMPG (1:1)	25	445	0.239	452	0.184
	50	444	0.144	443	0.108
DPPC:DMPG (1:2)	25	444	0.220	445	0.176
	50	443	0.147	446	0.125
DPPC:DMPG (2:1)	25	447	0.213	447	0.176
	50	437	0.143	437	0.116
DSPC:DMPG (5:1)	25	458	0.215	457	0.210
	50	458	0.200	457	0.196
DSPC:Ch:DSPE-PEG_{2000} (1:1:0.75)	25	440	0.216	448	0.185
	50	437	0.133	449	0.136

Upon increasing temperature, both compounds exhibit a significant decrease in fluorescence anisotropy (Table 6), feeling an increase in fluidity of the nanoliposome membranes at high temperature. Therefore, both compounds are mainly located in the nanoliposome membranes. The decrease in *r* values at 50 ºC is low in DSPC:DMPG (5:1) vesicles, due to the higher

melting transition temperature of DSPC (T_m = 55 ºC [13]), as this phospholipid is still in the gel phase at 50 ºC. This fact can also contribute to the more hydrated environment reported by these compounds in DSPC:DMPG liposomes, as the rigidity of these membranes can prevent the compounds to penetrate more deeper in the lipid membranes. Overall, these results indicate that both compounds can be transported in the hydrophobic region of the lipid bilayers.

4. Conclusions

New fluorescent methoxylated di(hetero)aryl ethers in the thieno[3,2-*b*]pyridine series, **2a-c**, were prepared by a copper-catalyzed Ullmann-type C-O coupling in moderate to good yields, using an amino acid as the ligand.

Cell growth inhibition assays showed that compounds **2a** and **2b** are promising as antitumoral drugs, presenting very low GI_{50} values in the three human tumor cell lines tested.

Both compounds have reasonable fluorescence quantum yields and can be considered as solvatochromic probes.

Our experimental results in nanoliposomes suggest that both compounds can be transported in the hydrophobic region of the lipid bilayer. The Egg-PC:Ch (7:3), Egg-PC:Ch:DMPG (7:3:1) and DSPC:Ch:DSPE-PEG2000 (1:1:0.75) nanoliposomes are the best formulations for encapsulation of these thienopyridines, considering the size (diameter lower than 100 nm) and polydispersity. These results may be important for future drug delivery applications of these new potential antitumoral arylетherthienopyridines, using nanoliposomes as drug carriers.

Acknowledgements

To the Foundation for the Science and Technology (FCT, Portugal) for financial support to the NMR portuguese network (PTNMR, Bruker Avance III 400-Univ. Minho). FCT and FEDER (European Fund for Regional Development) for financial support to the Research Centres, CQ/UM [PEst-C/QUI/UI0686/2011 (FCOMP-01-0124-FEDER-022716)] and CFUM [PEst-C/FIS/UI0607/2011 (F-COMP-01-0124-FEDER-022711)], and to the research projects PTDC/QUI/81238/2006 (FCOMP-01-0124-FEDER-007467) (photophysical studies) and PTDC/QUI-QUI/111060/2009 (F-COMP-01-0124-FEDER-015603) (organic synthesis and biological studies), which are also financed by COMPETE/QREN/EU.

References

[1] I. Hayakama, R. Shioya, T. Agatsuma, H. Furokawa, Y. Sugano, Thienopyridine and Benzofuran derivatives as potent anti-tumor agents possessing different structure-activity relationship, Bioorg. Med. Chem.14 (2004) 3411-3414.

[2] D.H. Boschelli, B. Wu, A.C.Barrios Sosa, H. Durutlic, J.J. Chen, Y. Wang, J.M. Golas, J. Lucas, F. Boscheli, Synthesis and Src kinase inhibitory activity of 2-phenyl- and 2-thienyl-7-phenylaminothieno[3,2-b]pyridine-6-carbonitriles, J. Med. Chem. 48 (2005) 3891-3902.

[3] S. Claridge, F. Raeppel, M.-C. Granger, N. Bernstein, O. Saavedra, L. Zhan, D. Llewellyn, A. Wahhab, R. Deziel, J. Rahil, N. Beaulieu, H. Nguyen, I. Dupont, A. Barsalou, C. Beaulieu, I. Chute, S. Gravel, M.-F. Robert, S. Lefebvre, M. Dubay, R. Pascal, J. Gillespie, Z. Jin, J. Wang, J.M. Besterman, A.R. MacLeod; A. Vaisburg, Discovery of a novel and potent series of thieno[3,2-b]pyridine-based inhibitors of c-Met and VEGFR2 tyrosine kinase, Bioorg. Med. Chem. Lett. 18 (2008) 2793-2798.

[4] S. Raeppel, S. Claridge, O. Saavedra, F. Gaudette, L. Zhan, M. Mannion, N. Zhou, F. Raeppel, M.-C. Granger, L. Isakovick, R. Deziel, H. Nguyen, N. Beaulieu, C. Beaulieu, I. Dupont, M.-F. Robert, S. Lefebvre, M. Dubay, J. Rahil, J. Wang, H. Ste-Croix, A. R. MacLeod, J.Besterman, A. Vaisburg, N-(3-fluoro-4-(2-arylthieno[3,2-b]pyridine-7-yloxy)phenyl)-2-oxo-3-phenylimidazolidine-1-carboxamides: a novel series of dual c-Met/VEGFR2 receptor tyrosine kinase inhibitors, Bioorg. Med. Chem. Lett. 19 (2009) 1323-1328.

[5] F. Gaudette, S. Raeppel, H. Nguyen, N. Beaulieu, C. Beaulieu, I. Dupont, A. Robert Macleod , J.M. Besterman, A. Vaisburg, Identification of potent and selective VEGFR receptor tyrosine kinase inhibitors having new amide isostere headgroups, Bioorg. Med. Chem. Lett. 20 (2010) 848-852.

[6] R. Banerjee, Liposomes: Applications in medicine, J. Biomater. Appl. 16 (2001) 3-21.

[7] Y. Malam, M. Loizidou, A. M. Seifalian, Liposomes and nanoparticles: nanosized vehicles for drug delivery in cancer, Trends in Pharmacol. Sci. 30 (2009) 592-599.

[8] R. C. Calhelha, M.-J. R. P. Queiroz, Synthesis of new thieno[3,2-*b*]pyridine derivatives by palladium-catalyzed couplings and intramolecular cyclizations, Tetrahedron Lett. 51 (2010) 281-283.

[9] P. Skehan, R. Storeng, D. Scudiero, A. Monks, J. McMahon, D. Vistica, J. T. Warren, H. Bokesch, S. Kenney, M. R. Boyd, New colorimetric cytotoxicity assay for anticancer-drug screening, J. Natl. Cancer Inst. 82 (1990) 1107-1112.

[10] A. Monks, D. Scudiero, P. Skehan, R. Shoemaker, K. Paull, D. Vistica, C. Hose, J. Langley, P. Cronise, A. Vaigro-Wolff, M. Gray-Goodrich, H. Campbell, J. Mayo, M. Boyd, Feasibility of a high-flux anticancer drug screen using a diverse panel of cultured human tumor-cell lines, J. Natl. Cancer Inst. 83 (1991) 757-776.

[11] B. R. Lentz, Membrane fluidity as detected by diphenylhexatriene probes, Chem. Phys. Lipids 50 (1989) 171-190.

[12] M. T. Lamy-Freund, K. A. Riske, The peculiar thermo-structural behavior of the anionic lipid DMPG, Chem. Phys. Lipids 122 (2003) 19-32.

[13] M. Ueno, S. Katoh, S. Kobayashi, E. Tomoyama, S. Ohsawa, N. Koyama, Y. Morita, Evaluation of phase transition temperature of liposomes by using the tautomerism of α-Benzoylacetoanilide, J. Coll. Interface Sci. 134 (1990) 589-592.

[14] E. Feitosa, P. C. A. Barreleiro, G. Olofsson, Phase transition in dioctadecyldimethylammonium bromide and chloride vesicles prepared by different methods, Chem. Phys. Lipids 105 (2000) 201-213.

[15] J.N. Demas, G.A. Crosby, Measurement of photoluminescence quantum yields – Review, J. Phys. Chem. 75 (1971) 991-1024.

[16] S. Fery-Forgues, D. Lavabre, Are fluorescence quantum yields so tricky to measure? A demonstration using familiar stationery products, J. Chem. Educ. 76 (1999) 1260.

[17] S. R. Meech, D. Phillips, Photophysics of some common fluorescence standards, J. Photochem. 23 (1983) 193-217.

[18] J. R. Lakowicz, Principles of Fluorescence Spectroscopy, Kluwer Academic/Plenum Press, New York, 1999.

[19] N. Mataga, T. Kubota, Molecular Interactions and Electronic Spectra, Marcel Dekker, New York, 1970.

[20] N. G. Bakhshiev, Universal molecular interactions and their effects on the position of the electronic spectra of molecules in two component solutions. I. Theory (liquid solutions), Opt. Spectrosc. 10 (1961) 379-384.

[21] N. G. Bakhshiev, Universal molecular interactions and their effects on the position of the electronic spectra of molecules in two component solutions, Opt. Spectrosc. 12 (1962) 309-313; Opt. Spectrosc. 13 (1962) 24-29.

[22] J. Lindley, Tetrahedron report number 163 : Copper assisted nucleophilic substitution of aryl halogen, Tetrahedron 40 (1984)1433-1456.

[23] L. D. Boger, A.M. Patane, J. Zhou, Total Synthesis of Bouvardin, O-Methylbouvardin, and O-Methyl-N9-desmethylbouvardin, J. Am. Chem. Soc.116 (1994) 8544-8556.

[24] D. Ma, Q. Cai, N,N-Dimethyl glycine-promoted Ulmann coupling reaction of phenols and aryl halides, Org. Lett. 5 (2003) 3799-3802.

[25] H. Zhang, Q. Cai, D. Ma, Amino acid promoted CuI-catalyzed C-N bond formation between aryl halides and amines or N-containing heterocycles, J. Org. Chem. 70 (2005) 5164-5174.

[26] M. R. Ranson, J. Carmichael, K. O'Byrne, S. Stewart, D. Smith, A. Howell, Treatment of advanced breast cancer with sterically stabilized liposomal doxorubicin: results of a multicenter phase II trial. J. Clin. Oncol. 15 (1997) 3185-3185.

[27] O. Lyass, B. Uziely, R. Ben-Yosef, D. Tzemach, N. I. Heshing, M. Lotem, G. Brufman, A. Gabizon, Correlation of toxicity with pharmacokinetics of pegylated liposomal doxorubicin (Doxil) in metastatic breast carcinoma, Cancer 89 (2000)1037-1047.

[28] M. E. R. O'Brien, N. Wigler, M. Inbar, R. Rosso, E. Grischke, A. Santoro, R. Catane, D. G. Kieback, P. Tomczak, S. P. Ackland, F. Orlandi, L. Mellars, L. Alland, C. Tendler, Reduced cardiotoxicity and comparable efficacy in a phase III trial of pegylated liposomal doxorubicin HCl (CAELYXTM/Doxil®) versus conventional doxorubicin for first-line treatment of metastatic breast cancer, Ann. Oncol. 15 (2004) 440-449.

[29] a) K. C. James, P. R. Noyce, Hydrogen bonding between testosterone propionate and solvent in chloroform-cyclohexane solutions, Spectrochim. Acta A 27 (1971) 691-696. b) G. R. Wiley, S. I. Miller, Thermodynamic parameters for hydrogen-bonding of chloroform with Lewis bases in cyclohexane - Proton magnetic-resonance study, J. Am. Chem. Soc. 94 (1972) 3287-3293.

[30] D. R. Lide (Ed.), Handbook of Chemistry and Physics, 83th Edition, CRC Press, Boca Raton, 2002.

[31] *Gaussian 09, Revision A.02*, M. J. Frisch, G. W. Trucks, H. B. Schlegel, G. E. Scuseria, M. A. Robb, J. R. Cheeseman, G. Scalmani, V. Barone, B. Mennucci, G. A. Petersson, H. Nakatsuji, M. Caricato, X. Li, H. P. Hratchian, A. F. Izmaylov, J. Bloino, G. Zheng, J. L. Sonnenberg, M. Hada, M. Ehara, K. Toyota, R. Fukuda, J. Hasegawa, M. Ishida, T. Nakajima, Y. Honda, O. Kitao, H. Nakai, T. Vreven, J. A. Montgomery, Jr., J. E. Peralta, F. Ogliaro, M. Bearpark, J. J. Heyd, E. Brothers, K. N. Kudin, V. N. Staroverov, R. Kobayashi, J. Normand, K. Raghavachari, A. Rendell, J. C. Burant, S. S. Iyengar, J. Tomasi, M. Cossi, N. Rega, J. M. Millam, M. Klene, J. E. Knox, J. B. Cross, V. Bakken, C. Adamo, J. Jaramillo, R. Gomperts, R. E. Stratmann, O. Yazyev, A. J. Austin, R. Cammi, C. Pomelli, J. W. Ochterski, R. L. Martin, K. Morokuma, V. G. Zakrzewski, G. A. Voth, P. Salvador, J. J. Dannenberg, S. Dapprich, A. D. Daniels, Ö. Farkas, J. B. Foresman, J. V. Ortiz, J. Cioslowski, and D. J. Fox, Gaussian, Inc., Wallingford CT, 2009.

[32] F. Jensen, in Introduction to Computational Chemistry, John Wiley & Sons, West Sussex, England, 1999.

[33] D. Papahadjopoulos, N. Miller, Phospholipid model membranes. I. Structural characteristics of hydrated liquid crystals., Biochim. Biophys. Acta 135 (1967) 624-638.

[34] K.A. Riske, L.Q. Amaral, H.-G. Döbereiner, M.T. Lamy, Mesoscopic structure in the chain-melting regime of anionic phospholipid vesicles: DMPG, Biophys. J. 86 (2004) 3722-3733.

[35] R.P. Barroso, K.R. Perez, I.M. Cuccovia, M.T. Lamy, Aqueous dispersions of DMPG in low salt contain leaky vesicles, Chem. Phys. Lipids, 165 (2012) 169-177.

[36] B. Valeur, Molecular Fluorescence - Principles and Applications, Weinheim, Wiley-VCH, 2002.

[37] M. R. Mozafari, V. Hasirci, Mechanism of calcium ion induced multilamellar vesicle DNA interaction. J. Microencapsul. 15 (1998) 55-65.

[38] Y. Ran, S.H. Yalkowsky, Halothane, a novel solvent for the preparation of liposomes containing 2-4'-amino-3'-methylphenyl benzothiazole (AMPB), an anticancer drug: A technical note, AAPS Pharm. Sci. Tech. 4 (2003) article 20.

[39] N. Berger, A. Sachse, J. Bender, R. Schubert, M. Brandl, Filter extrusion of liposomes using different devices: comparison of liposome size, encapsulation efficiency, and process characteristics, Int. J. Pharm. 223 (2001) 55-68.

[40] L. R. Tsuruta, A. M. Carmona-Ribeiro, Counterion effects on colloid stability of cationic vesicles and bilayer-covered polystyrene microspheres, J. Phys. Chem. 100 (1996) 7130-7134.

[41] E.M.S. Castanheira, M.S.D. Carvalho, A.R.O. Rodrigues, R.C. Calhelha, M.-J.R.P. Queiroz, New potential antitumoral fluorescent tetracyclic thieno[3,2-*b*]pyridine

derivatives: Interaction with DNA and nanosized liposomes, Nanoscale Res. Lett. 6 (2011) article 379.